Chemistry
A European
Journal

Chemistry Europe
European Chemical Societies Publishing

## Accepted Article

**Title:** Time Programmable Locking/Unlocking of the Calix[4]arene Scaffold by Means of Chemical Fuels

**Authors:** Stefano Di Stefano, Daniele Del Giudice, Emanuele Spatola, Roberta Cacciapaglia, Alessandro Casnati, Laura Baldini, and Gianfranco Ercolani



**To be cited as:** *Chem. Eur. J.* 10.1002/chem.202002574

**Link to VoR:** https://doi.org/10.1002/chem.202002574

WILEY-VCH

10.1002/chem.202002574

WILEY-VCH

FULL PAPER

# Time Programmable Locking/Unlocking of the Calix[4]arene Scaffold by Means of Chemical Fuels

Daniele Del Giudice,[a] Emanuele Spatola,[a] Roberta Cacciapaglia,[a] Alessandro Casnati,[b] Laura Baldini,*[b] Gianfranco Ercolani,*[c] and Stefano Di Stefano*[a]

[a] D. Del Giudice, E. Spatola, Dr. R. Cacciapaglia, Prof. S. Di Stefano
Dipartimento di Chimica
Università di Roma La Sapienza and ISB-CNR Sede Secondaria di Roma - Meccanismi di Reazione,
P.le A. Moro 5, I-00185 Roma, Italy.
E-mail: stefano.distefano@uniroma1.it

[b] Prof. A. Casnati, Prof. L. Baldini
Dipartimento di Scienze Chimiche, della Vita e della Sostenibilità Ambientale
Università degli Studi di Parma
Parco Area delle Scienze 17/A, 43124 Parma, Italy.
E-mail: laura.baldini@unipr.it

[c] Prof. G. Ercolani
Dipartimento di Scienze e Tecnologie Chimiche
Università di Roma Tor Vergata
Via della Ricerca Scientifica, 00133 Roma, Italy
E-mail: ercolani@uniroma2.it

Supporting information for this article is given via a link at the end of the document.

**Abstract:** Herein we report that 2-cyano-2-phenylpropanoic acid and its *p*-Cl, *p*-$CH_3$ and *p*-$OCH_3$ derivatives can be used as chemical fuels to control the geometry of the calix[4]arene scaffold in its cone conformation. It is shown that, under the action of the fuel, the cone calix[4]arene platform assumes a “locked” shape with two opposite aromatic rings strongly convergent and the other two strongly divergent (“pinched cone” conformation). Only when the fuel is exhausted, the cone calix[4]arene scaffold returns to its resting, “unlocked” shape. Remarkably, the duration of the “locked” state can be controlled at will by varying the fuel structure or amount. A kinetic study of the process shows that the consume of the fuel is catalyzed by the “unlocked” calixarene that behaves as an autocatalyst for its own production. A mechanism is proposed for the reaction of fuel consumption.

## Introduction

Modulation of the conformation of complex molecular architectures is one of the by-nature most used tool to control the chemical properties of biomolecules. In particular, chemically induced conformational changes are conveniently employed to modify binding capability or catalytic activity of allosteric proteins. Hemoglobin[1] or aspartate carbamoyltransferase[2] are famous and recurrently cited examples. In the case of man-made supramolecular systems, although involving far simpler structures, remarkable examples of chemically-induced conformational control of properties and reactivity have been reported, mainly based on molecular machines.[3,4] Among them our attention was directed to systems in which conformational changes are driven by chemical fuels.[5,6] In these cases, the conformational change, for example from state A to state B (A→B), and the consequent variation of chemical properties, persists as long as the fuel is present in solution and ends (B→A) when the fuel is exhausted.

Calix[4]arenes have been widely used as abiotic scaffolds in Supramolecular Chemistry thanks to the possibility of an easy functionalization of both rims with a large number of functional units. Importantly, in addition to the chemical functionalities of the appended units, the properties of calix[4]arene-based receptors or building blocks depend also on the conformational features of the scaffold. Even when blocked in one of the four possible structures (cone, partial cone, 1,2- and 1,3-alternate), the calixarene scaffold retains a certain degree of flexibility. A calix[4]arene in the cone geometry, for example, when functionalized at the lower rim with four alkyl or polyether chains (Figure 1, with R larger than $CH_3CH_2$—) rapidly interconverts between two equally stable pinched cone conformations where two distal aromatic rings are parallel to each other and the other two are tilted outwards.[7] This “breathing” movement is originated from a partial rotation around the eight Ar—$CH_2$ bonds and, as a consequence, the distances between the opposite carbon atoms $C_1$—$C_3$ and $C_2$— $C_4$ are coupled in such a way that when the former is at its minimum the latter is at its maximum and *vice-versa* (see Figure 1). When the calixarene is functionalized also at the upper rim, this equilibrium can be shifted towards one of the two possible pinched structures as a result of attractive or repulsive interactions between the upper rim distal substituents.[8,9,10] The consequences of this flexibility can be relevant on the calixarene properties, such as the availability of the aromatic cavity for guest complexation,[10] the macrocycle self-assembly properties[11] or the spectroscopic properties of calixarene-based dyes.[12,13] To the best of our knowledge, control on the conformational equilibrium of Figure 1 has been mainly attained through a change of the solvent,[10,12,14,15] a time-consuming operation that does not allow a fast switch between the two pinched cone structures. We figured that the use of a chemical fuel to induce the conformational change of the calixarene scaffold would be highly desirable as a convenient way to favour one of the two pinched cone structures in a time-controlled and programmable fashion without recurring to a variation of the solvent.

With the aim of controlling the conformational equilibrium of Figure 1 by means of the chemical fuels **1**,X (2-cyano-2-phenylpropanoic acid and its derivatives), which are known to be capable of driving the oscillatory movements of acid-base operated molecular machines,[5a,d,f,h,j,k,6] we hypothesized that 1,3-distal diaminocalix[4]arene **2**, could be a good candidate for our purpose. The inspiration came from our previous report on the

10.1002/chem.202002574




intramolecular Cannizzaro reaction occurring under basic conditions within the 1,3-distal diformylcalix[4]arene **3**.[16] Here, the intramolecular hydride transfer between the two aldehyde functions is strongly favored by the flexibility of the calixarene scaffold which allows the "H⁻" donor and acceptor functions to be in close proximity at transition state level as depicted in **4** (high Effective Molarity, EM[16a,17]). By the same token, protonation of compound **2** should result in the conjugate acid **2**H⁺ in which a strong intramolecular hydrogen bond binds the protonated amino group to the unprotonated one, forcing the two groups to be close to each other.

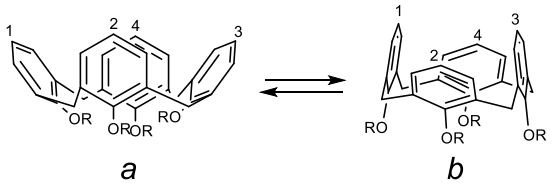


**Figure 1.** Conformational interconversion of a calix[4]arene in the cone structure (R > $CH_3CH_2$—) between two pinched cone conformations. The C1—C3 distance is at its maximum in conformation *a* and at its minimum in conformation *b*. The reverse holds for the C2—C4 distance.

Our design is illustrated in Figure 2. Reaction between fuels **1**,X and the "unlocked" calix[4]arene **2** (state **A**) would generate the ion pair **2**H⁺•ArC($CH_3$)C$NCO_2^-$ (state **B'**), which should possess a "locked" pinched-cone conformation with the two amino groups fixed in close proximity and the opposite unsubstituted aromatic nuclei far from each other. Subsequent decarboxylation and back proton transfer from **2**H⁺ to ArC($CH_3$)C$N^-$, which are intimately paired in state **B"**, would regenerate calixarene **2** in the unlocked resting state with compound **5** as a waste product closing the "conformational cycle". Thus, fuels **1**,X would serve to chemically control the conformational state of calixarene **2**.

## Results and Discussion

The four 2-ethoxyethoxy groups at the lower rim of 1,3-distal diaminocalix[4]arene **2** guarantee that the structure always maintains its cone conformation. $^1$H NMR spectrum in $CD_2Cl_2$ at 25 °C of 4.0 mM **2** is reported as the first trace from bottom of Figure 3. The pattern of this spectrum is that of a typical 1,3-distally disubstituted calix[4]arene in its cone conformation.

Addition of 1 mol equiv of fuel **1**,H immediately causes a series of shifts (compare the bottom trace and the second trace (t = 3 min), the latter being the first spectrum recorded after the addition of fuel) due to protonation of **2** (step **A**→**B'** in Figure 2). Signals marked in red and blue belonging to the aromatic rings

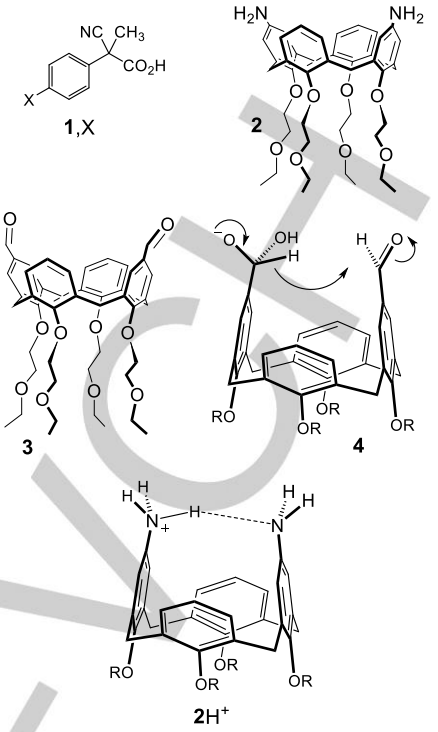


are shifted towards lower and higher fields, respectively. This witnesses the formation of ion pair **2**H⁺•ArC($CH_3$)C$NCO_2^-$ (state **B'**), with the calixarene scaffold assuming a rigid pinched cone conformation. The observed magnetic anisotropy is indeed typical of such conformation. The shifts of the signals marked in black belonging to the 2-ethoxyethoxy groups in the lower rim of the calixarene structure are also in accordance with the above conformational change

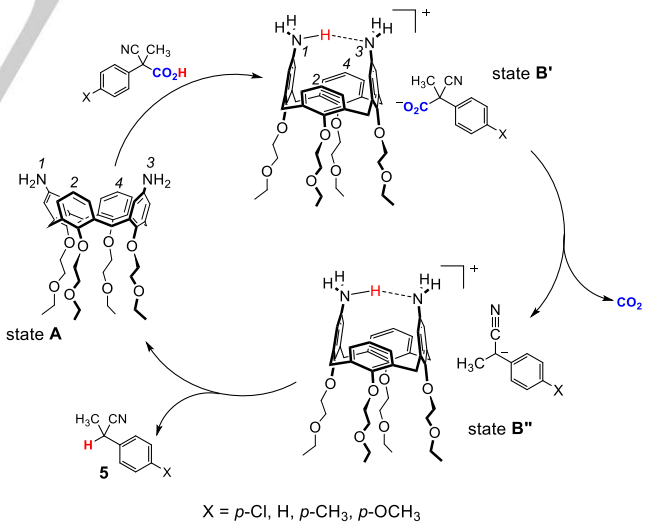


**Figure 2**. Proposed "conformational cycle" experienced by diaminocalix[4]arene **2** under the action of fuels **1**,X (see text).

.

10.1002/chem.202002574




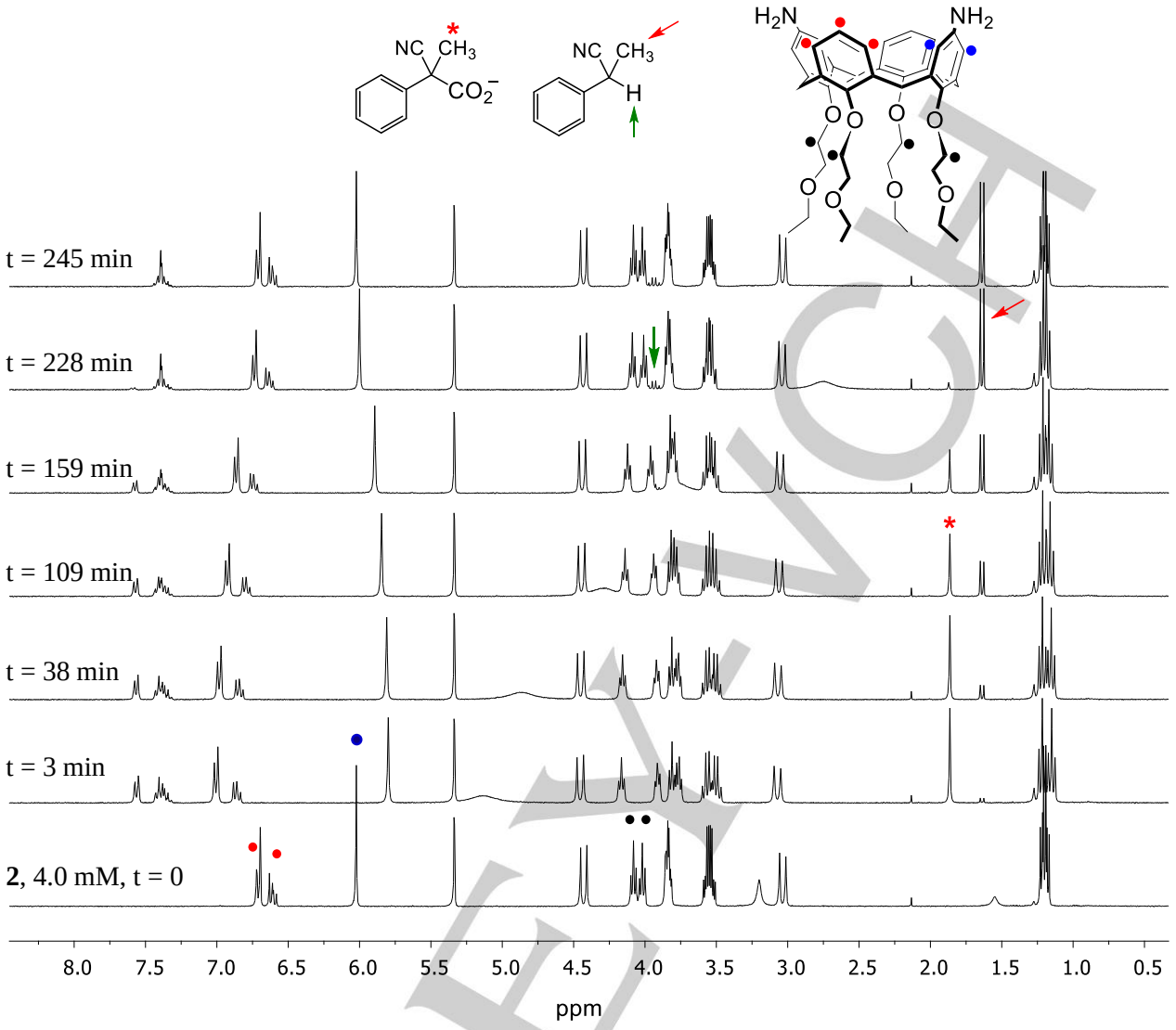


**Figure 3**. $^{1}$H NMR time-monitoring of the reaction between 4.0 mM **2** and 4.0 mM fuel **1**,H in $CD_2Cl_2$ at 25 °C. The bottom trace is the spectrum of 4.0 mM **2** taken before addition of the fuel

From 3 min ahead, decarboxylation and fast back proton transfer from **2**H$^+$ to ArC($CH_3$)CN$^-$ within the ion pair in state **B"** (Figure 2) regenerating the native unlocked cone conformation of **2** are apparent. At the end of the processes (t = 245 min) the solution only contains **2** in its native state **A** and the waste product **5**. Interestingly, proton exchange from **2** to **2**H$^+$ and *vice-versa* results to be fast on NMR time-scale. This finding contrasts with that obtained in the case of two previously reported molecular machines driven by fuel **1**,H, one based on a catenane[5a] and the other on a rotaxane[5e] structure. Moreover, in the present case, the absence of any signal ascribable to the ion pair **2**H$^+$•ArC($CH_3$)CN$^-$ (state **B"**) during the whole $^{1}$H NMR monitoring of the reaction, is in accordance with a very fast back proton transfer from **2**H$^+$ to ArC($CH_3$)CN$^-$.

The overall mechanism of the reaction **1**,H + **2** depicted in Figure 2, which is strongly supported by the NMR data of Figure 3, is definitely demonstrated by the fact that *para*-anisidine **6**, a monofunctional model compound for calixarene **2**, is not able to act as a base promoter of the decarboxylation of fuel **1**,H. A $CD_2Cl_2$ solution of 4.0 mM **1**,H and 8.0 mM **6** is recovered unaltered after 16 h at 25 °C (Figure S1), showing that the catalytic capability of **2** in promoting the decarboxylation of acid **1**,H, is dictated by an enhanced basicity of the amine functions of **2** when compared with that of the amine function of **6**. The possibility to share the proton between the two nitrogen atoms in the calixarene structure is a source of a basicity increase, which strongly resembles the topological enhancement of basicity found by Sauvage et al[18] and later by Di Stefano et al[5a] in the case of phenanthroline based catenanes.

The significantly higher basicity of **2** with respect to **6** is proved by the fact that after **2** is protonated with 1 mol equiv of trifluoroacetic acid (TFA) to give **2**H$^+$•$CF_3CO_2^-$, whose $^{1}$H NMR spectrum (Figure S2 top trace) is practically superimposable to calixarene signals of **2**H$^+$•ArC($CH_3$)C$NCO_2^-$ (state **B'**, trace at t = 3 min in Figure 3) addition of up to 50 mol equiv **6** (in water p$K_a$ = 5.36), fails in deprotonating **2**H$^+$•$CF_3CO_2^-$ (Figure S3). Deprotonation of **2**H$^+$•$CF_3CO_2^-$ is instead complete only after addition of 100 mol equiv of *N*,*N*-diethylaniline **7** (in water p$K_a$ = 6.57) (Figure S4). Remarkably, when **6** is protonated by TFA to give **6**H$^+$•$CF_3CO_2^-$, all aromatic signals are significantly

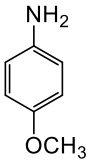

**6**

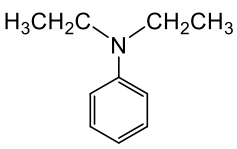

**7**

shifted to lower field (+0.23 ppm) as expected (Figure S5), in stark contrast with what occurs to the aromatic signal of the amino functionalized rings of **2**, which is shifted to higher fields (–0.22 ppm) upon conversion into **2**$H^+$•$CF_3CO_2^-$ by protonation. The shift to higher fields of the **2**$H^+$ signal is indeed suggestive of the switch of the scaffold conformation to a locked, closed pinched cone state. Indeed, in this structure, the two amino functionalized aromatic rings are parallel to each other as a consequence of the $NH_3^+\cdots NH_2$ intramolecular hydrogen bond and experience the shielding effect of the other two rings pointing outwards.

Eventually, VT NMR experiments performed on **2** and **2**$H^+$•$CF_3CO_2^-$ (Figure S6 and S7, respectively) showed minimal shifts ($\Delta\delta < 0.1$ ppm) of the signals in the temperature range -50°C ÷ 55°C and a slight broadening only at the low temperatures, indicating that the conformation of **2** both in the "unlocked" and in the "locked" state is not modified upon heating nor cooling.

**Kinetics and Mechanism of Decarboxylation**

The progress of the decarboxylation step **B'**→**B"**, which is the rate determining step of the whole motion cycle, can be monitored by $^1$H NMR as shown in Figure 3 ($CD_2Cl_2$). The reaction can be followed over time by monitoring either the disappearance of the reactant $ArC(CH_3)CNCO_2^-$, component of state **B'**, (Figure 4a), or the formation of the reaction product **5** (Figure 4b). The two measures are independent from each other since have been obtained by comparison of the areas of the corresponding methyl group signals with that of a calix[4]arene signal conveniently chosen. The carbanion $ArC(CH_3)CN^-$, component of state **B"**, was not detected during the entire reaction course, thus indicating that it is a reactive intermediate present at sub-detectable concentrations. The two kinetic profiles are in strict accordance, but instead of following the usual first-order behavior expected for the decarboxylation process,[5a,d,j] they present unusual features characteristic of a complex kinetics. In particular, it appears that the rate increases on increasing the extent of reaction with no sign of slowdown until the fuel is completely consumed, as evidenced by the sharp cusp in correspondence of the end of the reaction. An analogous profile is observed when the reaction in $CH_2Cl_2$ is monitored by UV-Vis spectrophotometry, by following the increase of absorbance at $\lambda = 315$ nm due to the higher molar absorptivity of the reaction products (Figure 4c and Figure S11).

A rate increase of the decarboxylation process on increasing the extent of reaction suggests that the process is catalyzed by the unprotonated calixarene **2** formed in the course of the reaction, that, in fact, behaves as an autocatalyst. Moreover, the cusp in the kinetic profiles is characteristic of a process which is pseudo zero-order in substrate, because any reaction order larger than zero would necessarily imply a slowdown of the reaction when the substrate concentration tends to zero. The operation of an autocatalytic process requires the presence of a background reaction capable of producing the initial amount of product that will then act as an autocatalyst for its own production. Taking into account the experimental results, it is reasonable to assume that the background reaction is the first-order decarboxylation process of the ion pair **2**$H^+$•$ArC(CH_3)CNCO_2^-$ (state **B'**), and that the main reaction is the calixarene assisted decarboxylation of state **B'** which is pseudo zero-order in substrate and first-order in the product **2** (Scheme 1).

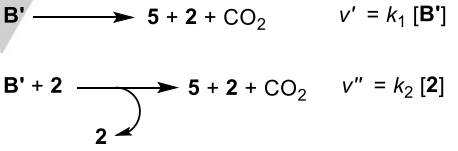


**Scheme 1.** Background and calixarene assisted decarboxylation reactions according to experimental results.

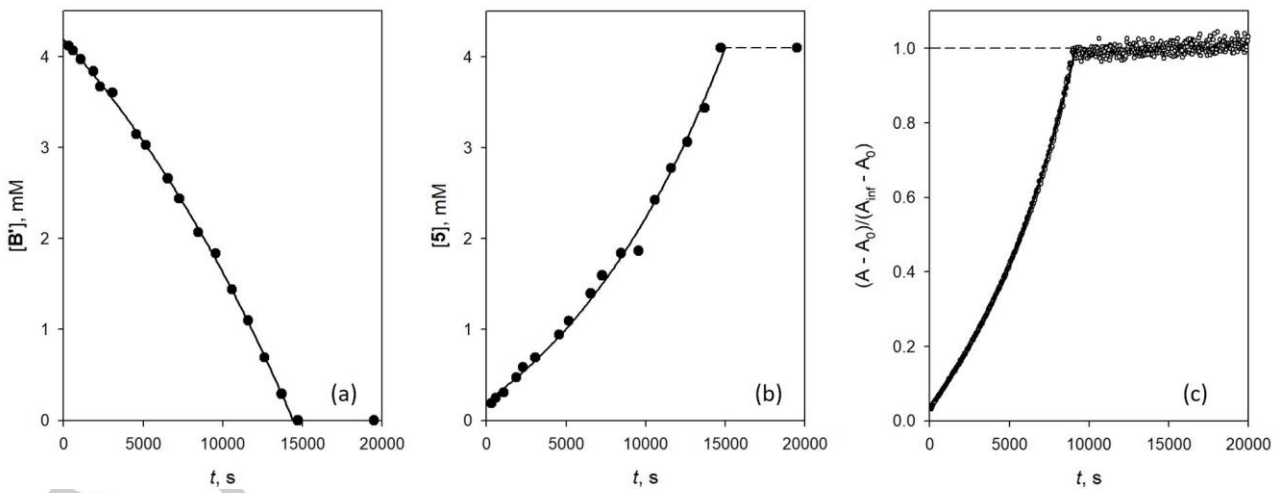


**Figure 4.** (a) Plot of the concentration of the $PhC(CH_3)CNCO_2^-$ component of state **B'** *vs*. time as monitored by $^1$H NMR for the reaction between 4.0 mM **2** and 4.0 mM fuel **1**,H in $CD_2Cl_2$ at 25 °C. The solid curve is the least-squares fit of the experimental points to the integral of Eq. 1 for the disappearance of **B'** (Eq. S6). (b) Plot of the concentration of product **5** *vs*. time for the same reaction of Figure 4a. The solid curve is the least-squares fit of the experimental points to the integral of Eq. 1 for product formation (Eq. S7). (c) Plot of the normalized absorbance at $\lambda = 315$ nm for the reaction between 1.0 mM **2** and 1.0 mM fuel **1**,H in $CH_2Cl_2$ at 25 °C. The solid curve is the least-squares fit of the experimental points to the integral of Eq. 1 for product formation (Eq. S7).

10.1002/chem.202002574




Accordingly, the rate equation for such scheme can be formulated as shown in Eq. 1, where *v'* is the rate of the background reaction, and *v''* is the rate of the autocatalytic process.

$$-\frac{d[\mathbf{B}']}{dt} = \frac{d[\mathbf{5}]}{dt} = \frac{d[\mathbf{2}]}{dt} = v' + v'' = k_1[\mathbf{B}'] + k_2[\mathbf{2}] \qquad (1)$$

The curves shown in Figures 4a-c were obtained by fitting the experimental points to the integrated rate equations, obtained as detailed in SI (pages S16-S18). The adherence of the calculated curve to the experimental points is very good, thus lending support to the above kinetic analysis.

Although Scheme 1 is in good agreement with the experimental data, the mechanism of the autocatalytic process is puzzling and needs to be clarified. The observation of a pseudo zero-order substrate dependency for a reaction occurring in homogeneous solution typically arises due to one of two possible mechanisms: *i*) the autocatalyst is involved in a rate-limiting process preceding the reaction with the substrate (the fuel); *ii*) the substrate is involved in a strong pre-equilibrium binding that saturates a catalytic species present in minute amounts, the resulting complex then reacts with the autocatalyst in the rate-limiting product formation. If mechanism *i* were operating, the rate of the autocatalytic process would be independent of the nature of the fuel. However, investigation of the kinetics of the reaction with different fuels **1**,X showed that the rate of the autocatalytic process is fuel-dependent (*vide infra*), thus ruling out mechanism *i,* and leaving mechanism *ii* as a viable option. The latter mechanism implies the presence of a catalytic species which, in all probability, can be attributed to an impurity of the solvent, since normalized kinetic profiles of reactions carried out at different dilution are practically superimposable (Figure S18). If the impurity had belonged to the reactants, its dilution would have slowed down the reaction. All commercial samples of methylene chloride are known to contain small amounts of metal ions of various charge, mostly present as chlorides. In such a low dielectric solvent, the anionic substrate $ArC(CH_3)CNCO_2^-$ is necessarily paired with a cation, and any of the resulting ion pairs must have a specific reactivity. It is reasonable to think that among the many cations present in solution, one or more of them not only displays a high affinity for the substrate but also gives an ion pair more reactive than $\mathbf{2}H^+ \bullet ArC(CH_3)CNCO_2^-$ (state **B'**). Since the autocatalytic reaction is first-order in the product **2**, the following mechanism can be envisaged for any cationic species, say $M^+$, present in solution (Scheme 2). The free calixarene **2** interacts with the ion pair $ArC(CH_3)CNCO_2^- \bullet M^+$ by coordinating the metal ion with the two aminic nitrogens. The coordination makes the carboxylate freer thus favoring the rate-limiting decarboxylation. The formed ion pair $ArC(CH_3)CN^- \bullet M^+$ quickly takes the proton from state **B'** giving the product **5** and the reactants, which begin a new catalytic cycle. Interestingly, when the reaction is carried out in the presence of trifluoroacetic acid (TFA) in the proportions **2** : **1**,H : TFA = 1 : 0.9 : 0.1, the kinetic profile changes as shown in Figure 5 where it appears that the autocatalytic reaction is slowed down, especially in the final part of the reaction where the product asymptotically approaches its final value. This evidence

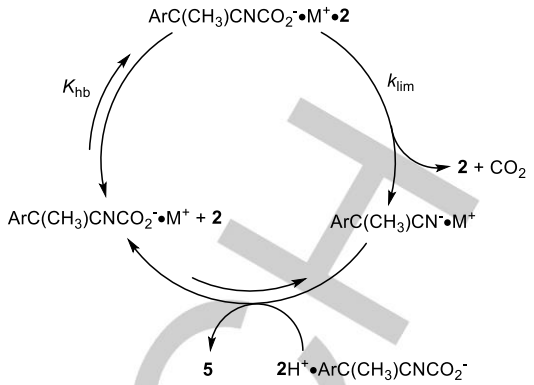


**Scheme 2.** Proposed kinetic mechanism involving the cationic impurity in the autocatalysis.

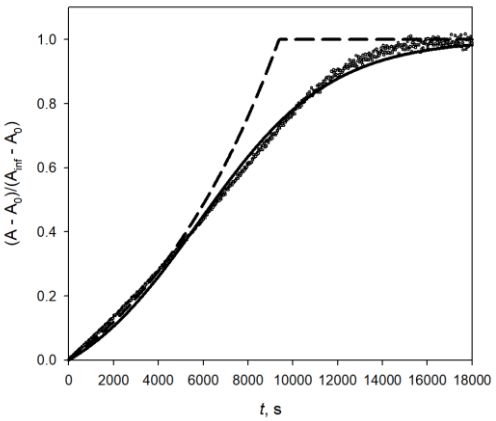


**Figure 5** Plot of the normalized absorbance at $\lambda$ = 315 nm for the reaction between 1.0 mM **2** and 0.9 mM fuel **1**,H in the presence of 0.1 mM TFA in $CH_2Cl_2$ at 25.0 °C. The points are experimental data, the dashed line has been calculated by the integral of Eq. 1 (Eq. S7) with $k_1$ and $k_2$ values obtained from the data in Figure 4c, and the solid line is the least-squares fit of the experimental points to the integral of Eq. 2 for product formation (Eq. S13).

suggests that now the autocatalytic process is first-order in substrate and first-order in the product **2**. Indeed, the experimental points have been successfully fitted by the integral rate equation obtained from Eq. 2 (SI, pages S19-S20).

$$-\frac{d[\mathbf{B}']}{dt} = \frac{d[\mathbf{5}]}{dt} = \frac{d[\mathbf{2}]}{dt} = k_1[\mathbf{B}'] + k_2[\mathbf{B}'][\mathbf{2}] \qquad (2)$$

This result can be explained by considering that both the conjugate bases of **1**,H and of TFA, initially in a 9:1 ratio, are present in solution. It is reasonable to assume that the two anions have similar chelating abilities toward metal ions, thus initially most of the catalytically active metal ion is ion paired with the conjugate base of **1**,H, and displays the usual catalytic mechanism. However, towards the end of the reaction, the conjugate base of TFA sequesters most of the catalytically active ion, and the mechanism of autocatalysis changes as it would be in the absence of catalytic impurities (Scheme 3), i.e. free calixarene **2** interacts by hydrogen bond with the ion pair $\mathbf{2}H^+ \bullet ArC(CH_3)CNCO_2^-$ (state **B'**) loosening the ion pair and favoring the rate-limiting decarboxylation.

10.1002/chem.202002574




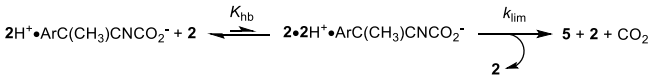


**Scheme 3**. Proposed mechanism of autocatalysis in absence of catalytic impurities.

Support for this mechanism is provided by the structures of models of the ion pair **2**H$^+$•ArC(CH$_3$)CNCO$_2^-$ (state **B'**) and of the ternary complex **2**•**2**H$^+$•ArC(CH$_3$)CNCO$_2^-$, fully optimized at the 2-layer ONIOM (ωB97XD/6-311+G(2d,p):HF/3-21G*) level of theory, including IEFPCM solvation in $CH_2Cl_2$, as implemented in Gaussian 16,[19] showing that the length of the hydrogen bond between the carboxylate anion and the ammonium ion changes from 1.547 Å to 1.614 Å on passing from the ion pair to the ternary complex (SI, Figure S19 pages S21-S26).

**Controlling the rate of the conformational cycle**

In spite of the above mechanistic complications, the rate with which the conformational cycle of the calix[4]arene scaffold occurs can be easily controlled by changing the nature of the *para*-substituent in the fuel aromatic moiety. As previously stated, the decarboxylation is the rate limiting step of the entire cycle of the conformational motion. Electron-withdrawing groups that stabilize the developing negative charge on the benzyl carbon atom in the decarboxylation transition state (TS), are indeed expected to accelerate the motion cycle, whereas electron-donating groups should retard it. This expectation is confirmed by the results obtained when acids **1**,*p*-Cl, **1**,*p*-CH$_3$ and **1**,*p*-OCH$_3$ are used as fuels to drive the conformational cycles of **2**. $^1$H NMR (Figure 7 and SI, pages S8-S10) and UV-Vis monitoring (SI, page S10) show exactly the same features of those related to the parent acid **1**,H, but the time needed to complete the cycle increases in the order **1**,*p*-Cl < **1**,H <**1**,*p*-CH$_3$ < **1**,*p*-OCH$_3$ (28, 250, 610, and 3200 min, respectively). Thus, a simple variation of the fuel structure allows to control the rate of the conformational motions of **2** exactly as in the case of the oscillating motions of acid-base operated molecular machines based on catenane or rotaxane structures.[5d,h,6]

Fit of the experimental points in Figure 6 to the integral of Eq. 1 for product formation (Eq. S7) gave the first-order rate constants $k_1$ and $k_2$ reported in Table 1.

Hammett plots of the rate constants $k_1$ and $k_2$ are linear with $\rho$ values equal to 3.6 and 4.2, respectively (Figure S20). The high $\rho$ values indicate that a significant fraction of the negative charge is developing on the benzylic carbon in both the transition states for the background and autocatalytic decarboxylation reactions. The slightly higher sensitivity observed for the autocatalytic process is in line with the formation of a looser ion pair.

A fine control of the rate of the conformational cycle of **2** can be obtained by controlling the amount of fuel added in solution. This trick was previously applied by Leigh et al[5i] to modulate the time in which a rotaxane-based machine, working as a dissipative catalyst, persists in one of the two available co-conformations. As an example, Figure 7 reports the $^1$H-NMR monitoring of the **1**,H + **2** reaction progress at different relative concentrations of the two reactants. Concentration of **2** is fixed at 4.0 mM while concentration of **1**,H is 4.0 mM (black trace), 5.4 mM (red trace), or 8.0 mM (green trace). It is evident that excess of fuel with respect to **2** retards the recovery of the resting conformation of the neutral calixarene **2**, increasing the life time of the pinched cone conformation of **2**H$^+$.[20]

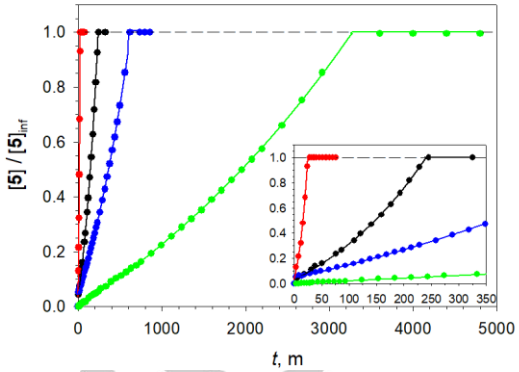


**Figure 6**. Plot of the concentration of the product **5** vs. time as monitored by $^1$H NMR for the reaction between 4.0 mM **2** and 4.0 mM fuel **1**,p-Cl (red trace), 4.0 mM **2** and 4.0 mM fuel **1**,H (black trace), 4.0 mM **2** and 4.0 mM fuel **1**,p-CH$_3$ (blue trace) and 3.6 mM **2** and 3.6 mM fuel **1**,p-OCH$_3$ (green trace), in $CD_2Cl_2$ at 25 °C. The solid curve is the least-squares fit of the experimental points to the integral of Eq. 1 for product formation (Eq. S7). Since protonation of **2** by ArC(CH$_3$)CNCO$_2$H (**A**→**B'**) and re-protonation of ArC(CH$_3$)CN$^-$ by **2**H$^+$ (**B"**→**A**) are very fast reactions, each trace describes the corresponding, complete **A**→**B'**→**B"**→**A** cycle. For the corresponding sequences of $^1$H NMR spectra see SI, pages S8-S10.

**Table 1.** First-order rate constants $k_1$ and $k_2$ for the reactionof different fuels **1**,X according to Scheme 1 and Eq. 1

| X | $k_1$, s$^{-1}$ | $k_2$, s$^{-1}$ |
|---|---|---|
| *p*-Cl | $(2.9 \pm 0.4) \times 10^{-4}$ | $(1.2 \pm 0.1) \times 10^{-3}$ |
| H | $(3.2 \pm 0.1) \times 10^{-5}$ | $(1.2 \pm 0.1) \times 10^{-4}$ |
| *p*-CH$_3$ | $(1.6 \pm 0.1) \times 10^{-5}$ | $(3.8 \pm 0.1) \times 10^{-5}$ |
| *p*-OCH$_3$ | $(3.3 \pm 0.1) \times 10^{-6}$ | $(7.3 \pm 0.1) \times 10^{-6}$ |

As also observed in the case of a catenane based molecular machine,[5a,f,j] when an excess of fuel is present, the latter is very probably associated with the carboxylate forming a ternary complex RCO$_2^-$•HO$_2$CR•**2**H$^+$, whose structure is analogous to a solvent separated ion pair. The latter association weakens the ion pairing with **2**H$^+$, and this is very likely the reason why, at the beginning of the reaction, the signal related to the protons of amino substituted aromatic rings in **2**H$^+$ are found at lower fields than expected (5.82 and 5.85 ppm for the red and green trace, respectively, to be compared with 5.80 for the black trace; Figure 8).

The kinetic behavior of the reaction in the presence of an excess of fuel is not trivial and requires some comment. It is evident that free calixarene **2** cannot be present with an excess of fuel because it would be immediately protonated by the latter as soon as it forms. Accordingly, under this condition the autocatalytic reaction cannot work because there is no free calixarene **2** available. On the other hand, depending on the amount of excess fuel, two first-order decarboxylation reactions can be envisaged, one due to the ion pair **2**H$^+$•RCO$_2^-$ (state **B'**), and the other due to the ternary complex RCO$_2^-$•HO$_2$CR•**2**H$^+$. In both cases, immediately after decarboxylation of ArC(CH$_3$)CNCO$_2^-$, the just formed carbanion ArC(CH$_3$)CN$^-$ will take the proton from the stronger acid RCO$_2$H in excess rather than from **2**H$^+$, which will persist in its protonated form (pinched

10.1002/chem.202002574


cone conformation). Thus, the result of both the two decarboxylation reactions consists of the depletion of the ternary complex in favor of state **B'** (Eq. 3) until all the fuel $RCO_2H$ in excess is consumed. This point corresponds to the minimum of

$$RCO_2^- \bullet HO_2CR \bullet \mathbf{2}H^+ \longrightarrow RH + CO_2 + \mathbf{2}H^+ \bullet RCO_2^- \qquad (3)$$

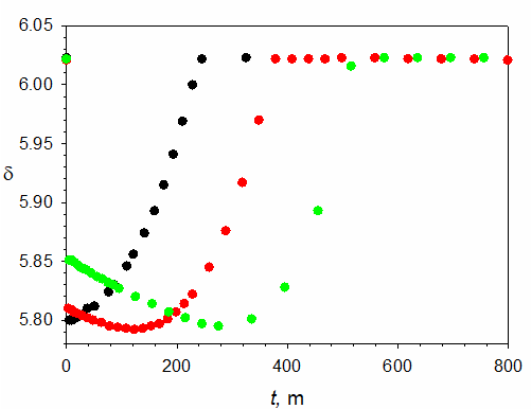


**Figure 7**. Controlling the duration of the conformational cycle of the calix[4]arene scaffold of **2** (4.0 mM) by regulating the excess of fuel **1**,H (4.0 mM black trace, 5.4 mM red trace, 8.0 mM green trace). $^1$H NMR monitoring of the chemical shift of protons on the amino-substituted aromatic rings ($CD_2Cl_2$ 25 °C). For related sequences of $^1$H NMR spectra see Figure 3 and SI, pages S13-S14.

the curves shown in Figure 7, that in turn corresponds to the chemical shift of the signal of the ion pair **2**$H^+$•$RCO_2^-$, state **B'** (δ = 5.80 ppm for both red and green traces). Note that from this point on, the reaction proceeds according to Scheme 1, where the first-order decarboxylation reaction of state **B'** is accompanied by the autocatalytic process. Indeed, the ascending portions of the curves are parallel to each other, indicating that after the minimum the same process is occurring. Since the excess fuel can be controlled at will, one has a full control over the time spent by the calixarene scaffold in the pinched cone conformation.

## Conclusion

In this report we have shown that the shape of a calix[4]arene scaffold in its cone conformation can be controlled by the use of chemical fuels. In particular, the cone 1,3-distal isomer of the upper rim functionalized diaminocalix[4]arene **2** offers a unique solution for this purpose. The basicity of the system is indeed enhanced by the chance of the two amino functions to share the proton in the conjugate acid. This basicity enhancement enables the diaminocalix[4]arene to promote the decarboxylation of a series of activated acids **1**,X, which act as chemical fuels. During the decarboxylation reaction the vast majority of the calixarene molecules persists in the closed pinched cone conformation with the two amino groups convergent and the two opposite distal positions strongly divergent (locked state). The time spent by the calix[4]arene scaffold in the locked state can be regulated by the choice of the fuel used to drive the conformational cycle, and finely modulated by controlling the amount of added fuel.

We believe that the possibility to fine-tune the conformational interconversion of the calixarene in a time dependent fashion and without recurring to solvent changes opens the way to new perspectives in calixarene chemistry, ranging from molecular receptors to sensing devices whose active state could be switched on at will.[21]

## Experimental Section

**Instrument and methods:** $^1$H NMR spectra were recorded on a 300 MHz spectrometer. The spectra were internally referenced to the residual proton signal of the solvent at 5.30 ppm. VT $^1$H NMR spectra were recorded on a 600 MHz spectrometer. All the experiments were carried out in thermostated NMR tubes. UV–Vis measurements were performed on a Perkin Elmer Lambda 18 spectrophotometer.

**Materials:** All reagents and solvents were purchased at the highest commercial quality and were used without further purification, unless otherwise stated. $CH_2Cl_2$ and $CD_2Cl_2$ were dried over molecular sieves (3 Å) for 24 h and stored in a desiccator loaded with activated silica gel Rubin. Before use the molecular sieves were activated at 300 °C for 24 h. Fuels **1**,X[5d] and 1,3-diaminocalix[4]arene **2**[22] were available from previous investigations.

**NMR decarboxylation experiment of fuel 1,X in the presence of 4.0 mM calix[4]arene 2:** In a typical NMR decarboxylation experiment, 1.78 mg of calix[4]arene **2** were weighed into an NMR tube and diluted with $CD_2Cl_2$ giving a solution ~ 4.0 mM. The t = 0 $^1$H NMR spectrum was recorded and then an aliquot of a stock solution of **1**,X was added so that the final volume of the solution was 600 µl. Thus, concentration of calix[4]arene **2** was 4.0 mM, that of fuel **1**,X was 4.0 mM or higher for the experiments with excess of fuel.

**UV-vis decarboxylation experiments of fuel 1,X in presence of 0.30 mM calix[4]arene 2:** In a typical UV-vis decarboxylation experiment, 200 µl of a 3.0 mM stock solution of calix[4]arene **2** and an aliquot of a stock solution of fuel **1**,X were mixed in a 1.0 cm path length cuvette at 25 °C. Then, the solution was diluted with $CD_2Cl_2$ so that the final volume was 2.00 mL, fixing the concentration of calix[4]arene **2** to 0.30 mM and that of fuel **1**,X to 0.30 mM for equimolar experiments, or higher for the experiments with excess of fuel.

**NMR titrations of 2$H^+$•$CF_3CO_2^-$:** Calix[4]arene **2** (0.89 mg) was weighed into an NMR tube and diluted with 575 µl $CD_2Cl_2$ to give a 2.1 mM solution. Then, 20 µl of a 0.06 M stock solution of TFA were added to the solution giving a ~ 2.0 mM solution of **2**$H^+$•$CF_3CO_2^-$. At this point, subsequent aliquots of 5.0 µl of a 0.06 M stock solution of *p*-anisidine **6** were added up to 50 mol equiv NMR spectra of the solution were recorded at each titrant addition. In another experiment, aliquots of a stock solution of N,N-diethylaniline **7** were added to a ~ 2.0 mM **2**$H^+$•$CF_3CO_2^-$ solution in the NMR tube, prepared as described before, until 100 mol equiv of the titrant were added.

## Acknowledgements

This work was supported by University of Roma La Sapienza (Progetti di Ricerca Grandi 2018, prot. n. RG1181641DCAAC4E) and by the Italian Ministry of Instruction, University and Research programmes (COMP-HUB initiative, Departments of Excellence Program and PRIN 2017E44A9P). "Centro Interfacoltà di Misure" (CIM) of the University of Parma is acknowledged for VT-NMR experiments.

**Keywords:** Calixarene • Chemical Fuel • Molecular Motions • Conformational Control • Molecular Machine

[1] M.-R. Mihailescu, I. M. Russu, *Proc. Natl. Acad. Sci. USA* **2001**, *98*, 3773-3777.

[2] W. N. Lipscomb, *Adv. Enzymol. Relat. Areas Mol. Biol.* **1994**, *68*, 67–151.

[3] (a) S. Erbas-Cakmak, D. A. Leigh, C. T. McTernan, A. L. Nussbaumer, *Chem. Rev*. **2015**, *115*, 10081–10206; (b) V. Blanco, D. A. Leigh, V. Marcos, *Chem. Soc. Rev*. **2015**, *44*, 5341–5370; (c) M. Vlatkovic, B. S. L. Collins, B. L. Feringa, *Chem. Eur. J*. **2016**, *22*, 17080–17111; (d) L. van Dijk, M. J. Tilby,R. Szpera, O. A. Smith, H. A. Bunce, S. P. Fletcher, *Nat. Chem. Rev*. **2018**, *2*, 0117; (e) M. Baroncini, L. Casimiro, C. de Vet, J. Groppi, S. Silvi,A. Credi, *ChemistryOpen* **2018**, *7*, 169–179; (f) M. Baroncini, S. Silvi A. Credi, *Chem. Rev.* **2020**, *120*, 200–268.

[4] Molecular machine based switchable catalysts are particularly interesting. Selected examples are (a) J. Wang, B. L. Feringa, *Science* **2011**, *331*, 1429–1432; (b) V. Blanco, A. Carlone, K. D. Hänni, D. A. Leigh, B. A. Lewandowski, *Angew. Chem. Int. Ed*. **2012**, *51*, 5166–5169; (c) J. Beswick, V. Blanco, G. De Bo, D. A. Leigh, U. Lewandowska, B. A. Lewandowski, K. Mishiro, *Chem. Sci*. **2015**, *6*, 140–143; (d) M. Galli, J. E. M. Lewis, S. M Goldup, *Angew. Chem. Int. Ed*. **2015**, *54*, 13545–13549; (e) C. S. Kwan, A. S. C. Chan, K. C. -F. Leung, *Org. Lett*. **2016**, *18*, 976–979; (f) N. Mittal, S. Pramanik, I. Paul, S. De, M. Schmittel, *J. Am. Chem. Soc*. **2017**, *139*, 4270–4273; (g) S. Semwal, J. Choudhury, *Angew. Chem. Int. Ed*. **2017**, *56*, 5556–5560; (h) K. Eichstaedt, J. Jaramillo-Garcia, D. A. Leigh, V. Marcos, S. Pisano, T. A. Singleton, *J. Am. Chem. Soc*. **2017**, *139*, 9376–9381; (i) G. De Bo, D. A. Leigh, C. T. McTernan, S. A. Wang, *Chem. Sci*. **2017**, *8*, 7077–7081; (j) J. Y. C. Lim, N. Yuntawattana, P. D. Beer, C. K. Williams, *Angew. Chem. Int. Ed*. **2019**, *58*, 6007–6011; *Angew. Chem.* 2019, **131**, 6068–6072.

[5] (a) J. A. Berrocal, C. Biagini, L. Mandolini, S. Di Stefano, *Angew. Chem. Int. Ed.* **2016**, *55*, 6997–7001; (b) M. R. Wilson, J. Solà, A. Carlone, S. M Goldup, N. Lebrasseur D. A. Leigh, *Nature* **2016**, *534*, 235–240; (c) S. Erbas-Cakmak, S. D. P. Fielden, U. Karaca, D. A. Leigh, C. T. McTernan, D. J. Tetlow, M. R. Wilson, *Science* **2017**, *358*, 340–343; (d) C. Biagini, S. Albano, R. Caruso, L. Mandolini, J. A. Berrocal and S. Di Stefano, *Chem Sci.* **2018**, *9*, 181–188; (e) A. Ghosh, I. Paul, M. Adlung, C. Wickleder, M. Schmittel, *Org. Lett.* **2018**, *20*, 1046−1049; (f) C. Biagini, F. Di Pietri, L. Mandolini, O. Lanzalunga, S. Di Stefano, *Chem. Eur. J.* **2018**, *24*, 10122–10127; (g) Q. Shi, C.-F. Chen, *Chem. Sci.* **2019**, *10*, 2529–2533; (h) P. Franchi, C. Poderi, E. Mezzina, C. Biagini, S. Di Stefano, M. Lucarini, *J. Org. Chem.* **2019**, *84*, 9364−9368; (i) C. Biagini, S. P. Fielden, D. A. Leigh, F. Schaufelberger, S. Di Stefano, D. Thomas, *Angew. Chem. Int. Ed.* **2019**, *58*, 9876 –9880; (j) C. Biagini, G. Capocasa, V. Cataldi, D. Del Giudice, L. Mandolini and S. Di Stefano, *Chem. Eur. J.* **2019**, *25*, 15205–15211; (k) C. Biagini, G. Capocasa, V. Cataldi, D. Del Giudice, L. Mandolini and S. Di Stefano, *Org. Biomol. Chem.* **2020**, *18*, 3867–3873.

[6] C. Biagini, S. Di Stefano, *Angew. Chem. Int. Ed.* **2020**, *59*, 8344– 8354.

[7] A. Arduini, M. Fabbi, M. Mantovani, L. Mirone, A. Pochini, A. Secchi, R. Ungaro, *J. Org. Chem.* **1995**, *60*, 1454–1457.

[8] J. Scheerder, R. H. Vreekamp, J. F. J. Engbersen, W. Verboom, J. P. M. Van Duynhoven, D. N. Reinhoudt, *J. Org. Chem.* **1996**, *61*, 3476–3481.

[9] F. C. Krebs, M. Larsen, M. Jørgensen, P. R. Jensen, M. Bielecki, K. Schaumburg, *J. Org. Chem.* **1998**, *63*, 9872–9879.

[10] M. Lazzarotto, F. Sansone, L. Baldini, A. Casnati, P. Cozzini, R. Ungaro, *Eur. J. Org. Chem.* **2001**, *3*, 595–602.

[11] L. Baldini, F. Sansone, G. Faimani, C. Massera, A. Casnati, R. Ungaro, *Eur. J. Org. Chem.* **2008**, *5*, 869–886.

[12] I. Tosi, M. Segado Centellas, E. Campioli, A. Iagatti, A. Lapini, C. Sissa, L. Baldini, C. Cappelli, M. Di Donato, F. Sansone, F. Santoro, F. Terenziani, *ChemPhysChem* **2016**, *17*, 1686–1706.

[13] B. Bardi, I. Tosi, F. Faroldi, L. Baldini, F. Sansone, C. Sissa, F. Terenziani, *Chem. Commun.* **2019**, *55*, 8098–8101.

[14] M. Jørgensen, M. Larsen, P. Sommer-Larsen, W. Batsberg Petersen, H. Eggert, *J. Chem. Soc. Perkin Trans. 1* **1997**, *19*, 2851–2855.

[15] F. Sansone, E. Chierici, A. Casnati, R. Ungaro, *Org. Biomol. Chem.* **2003**, *1*, 1802–1809.

[16] (a) M. Galli, J. A. Berrocal, S. Di Stefano, R. Cacciapaglia, L. Mandolini, L. Baldini, A. Casnati, F. Ugozzoli, *Org. Biomol. Chem.* **2012**, *10*, 5109–5112; (b) M. Ciaccia, I. Tosi, R. Cacciapaglia, A. Casnati, L. Baldini, S. Di Stefano, *Org. Biomol. Chem.* **2013**, *11*, 3642–3648; (c) J. A. Berrocal, M. B. Baker, L. Baldini, A. Casnati, S. Di Stefano, *Org. Biomol. Chem.* **2018**, *16*, 7255–7264.

[17] For a general discussion on EM see: (a) S. Di Stefano, L. Mandolini, *Phys. Chem. Chem. Phys.* **2019**, *21*, 955-987; (b) S. Di Stefano, G. Ercolani, *Adv. Phys. Org. Chem.* **2016**, *50*, 1–76; (c) P. Motloch, C. A. Hunter, *Adv. Phys. Org. Chem.* **2016**, *50*, 77-118.

[18] M. Cesario, C. O. Dietrich-Buchecker, A. Edel, J. Guilhem, J.-P. Kintzinger, C. Pascard, J.-P. Sauvage, *J. Am. Chem. Soc.* **1986**, *108*, 6250–6254.

[19] Gaussian 16, Revision C.01, Frisch, M. J. *et al.* Gaussian, Inc., Wallingford CT, 2019.

[20] A coherent scenario is observed when the reactions are monitored by UV-Vis spectroscopy (see SI, page S15). Furthermore, the same effects are also observed when excess amounts of the fuel **1**,*p*-Cl are added to **2** (see SI, page S15).

[21] To illustrate the principle more in details, let us consider a functional group G which is active (recognition, catalysis, transport) in the unpaired form and deactivated in the paired form (G:::G). If a cone calix[4]arene is functionalized at the upper rim with two amino groups in the 1,3 distal positions and with two groups G in the opposite 2,4 positions in such a way that the two groups G are paired in the resting state, an OFF/ON/OFF system can be realized in which the addition of the fuel causes the fixation of the pinched cone conformation with functional groups G unpaired and consequently activated until fuel exhaustion.

[22] L. Baldini, R. Cacciapaglia, A. Casnati, L. Mandolini, R. Salvio, F. Sansone, R. Ungaro, *J. Org. Chem.* **2012**, *77*, 3381-3389.

10.1002/chem.202002574

WILEY-VCH



## Entry for the Table of Contents

FULL PAPER

The shape of the cone calix[4]arene scaffold can be controlled by means of chemical fuels. The time in which the calix[4]arene platform persists in the "locked" shape is controlled by varying nature and amount of the chemical fuel.

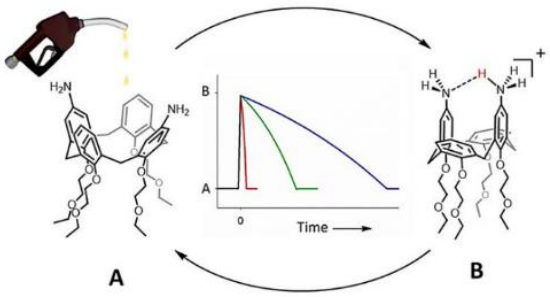


*Daniele Del Giudice, Emanuele Spatola, Roberta Cacciapaglia, Alessandro Casnati Laura Baldini,* Gianfranco Ercolani,* and Stefano Di Stefano**

***Page No. – Page No.***

**Time Programmable Locking/Unlocking of the Calix[4]arene Scaffold by Means of Chemical Fuels**